Scientific Reports

https://doi.org/10.1038/s41598-026-38605-5

Article in Press

Genome editing across Dictyostelia species enables comparative functional genetics of social amoebas

Received: 24 November 2025

Accepted: 30 January 2026

Published online: 05 February 2026

Cite this article as: Oishi S., Doi S., Sekida T. *et al.* Genome editing across Dictyostelia species enables comparative functional genetics of social amoebas. *Sci Rep* (2026). https://doi.org/10.1038/s41598-026-38605-5

Shuka Oishi, Sousuke Doi, Takumi Sekida, Kensuke Yamashita, Yoko Yamada & Tetsuya Muramoto

We are providing an unedited version of this manuscript to give early access to its findings. Before final publication, the manuscript will undergo further editing. Please note there may be errors present which affect the content, and all legal disclaimers apply.

If this paper is publishing under a Transparent Peer Review model then Peer Review reports will publish with the final article.

ARTICLE IN PRESS

© The Author(s) 2026. **Open Access** This article is licensed under a Creative Commons Attribution-NonCommercial-NoDerivatives 4.0 International License, which permits any non-commercial use, sharing, distribution and reproduction in any medium or format, as long as you give appropriate credit to the original author(s) and the source, provide a link to the Creative Commons licence, and indicate if you modified the licensed material. You do not have permission under this licence to share adapted material derived from this article or parts of it. The images or other third party material in this article are included in the article's Creative Commons licence, unless indicated otherwise in a credit line to the material. If material is not included in the article's Creative Commons licence and your intended use is not permitted by statutory regulation or exceeds the permitted use, you will need to obtain permission directly from the copyright holder. To view a copy of this licence, visit http://creativecommons.org/licenses/by-nc-nd/4.0/.

ARTICLE IN PRESS

Genome editing across Dictyostelia species enables comparative functional genetics of social amoebas

Shuka Oishi, Sousuke Doi, Takumi Sekida, Kensuke Yamashita, Yoko Yamada, Tetsuya Muramoto*

Department of Biology, Faculty of Science, Toho University, 2-2-1 Miyama, Funabashi, Chiba, 274-8510 Japan.

*Corresponding author:
tetsuya.muramoto@sci.toho-u.ac.jp

ARTICLE IN PRESS

ARTICLE IN PRESS

Abstract

Gene manipulation is essential for understanding biological mechanisms, yet genetic modification in the social amoebas (Dictyostelia) has been largely limited to *Dictyostelium discoideum*. Here, we aimed to establish a CRISPR/Cas9-based genome-editing system applicable across the phylogenetic breadth of Dictyostelia, spanning Groups 1–4. Using an extrachromosomal CRISPR/Cas9 vector from *D. discoideum*, we disrupted *stlA* and *pkaC* in *Polysphondylium violaceum* and *pkaC* in two early-branching species, *Heterostelium pallidum* and *Cavenderia fasciculata*. In *D. discoideum*, co-introduction of donor oligos with the CRISPR vector enabled selection-free knockout generation of *pkaC* with 28.6% efficiency. In *H. pallidum*, where genome editing is typically inefficient, co-electroporation of donor oligos with the CRISPR/Cas9 vector followed by 4 days of drug selection increased the frequency of *pkaC* disruption from 0.9% to 8.3%. These results demonstrated that the *D. discoideum* CRISPR/Cas9 system can be extended across Dictyostelia, providing a versatile platform for comparative genetic and evolutionary developmental studies.

Keywords: *Dictyostelium*; dictyostelids; CRISPR-Cas9; genome editing; multicellular development; cell-type differentiation

ARTICLE IN PRESS

Introduction

Social amoebas (Dictyostelia) are a monophyletic group of eukaryotic microorganisms characterized by aggregative multicellularity, which is a distinctive form of multicellular organization that has evolved independently in multiple eukaryotic lineages [1,2]. Under nutrient-rich conditions, solitary amoebas feed on bacteria and proliferate independently as single cells. When starved, these amoebas communicate through species-specific chemoattractant signals, such as cyclic AMP (cAMP) in *Dictyostelium discoideum* and glorin or other compounds in early-branching species, to aggregate and form multicellular structures known as fruiting bodies. Within these structures, cells undergo coordinated differentiation into two major types: spores, which ensure survival and dispersal, and stalk cells, which undergo terminal differentiation and die to elevate and release spores [3,4]. This division of labor serves as a powerful model for examining the evolution of cooperation and emergence of specialized cell types during the transition to multicellularity.

Dictyostelia diverged into four major evolutionary groups (Groups 1–4), which

ARTICLE IN PRESS

differ markedly in their morphogenesis, cell-type specialization, and signaling systems. Phylogenomic analyses based on conserved protein datasets place the root between Groups 1+2 and Groups 3+4, revealing stepwise evolutionary transitions in multicellular organization [5-7]. Comparative reconstructions further indicate that ancestral groups retain the ability to encyst and form relatively simple fruiting structures, whereas Group 4 species lost encystation ability and evolved pronounced cell-type differentiation, including the formation of specialized supporting cells such as cup cells and basal disc cells [2]. Comparative genomics and transcriptomics have provided important insights into the expansion of developmental complexity in Dictyostelia. Genome sequencing across all major groups has enabled the identification of conserved and lineage-specific gene repertoires underlying developmental signaling [8,9], whereas RNA-seq analyses have revealed extensive rewiring of developmental gene expression programs among phylogenetically distant species [10,11]. Beyond comparative gene content and transcriptional profiles, functional studies have begun to connect comparative datasets to developmental mechanisms. For example, knockout analyses of the ancestral *cdl1* gene have demonstrated its conserved role in core developmental processes, whereas Group-4-specific duplicates have functionally diverged to support novel cell-type specializations [12]. Despite these advances, the functional genetics of Dictyostelia remain limited. Homologous recombination is well-developed only in *D. discoideum*, and although gene disruption has been achieved in species such as *Heterostelium pallidum* (formerly *Polysphondylium pallidum*) and *Polysphondylium violaceum*, these methods have not yet been widely adopted or consistently applied [13,14]. This technical limitation continues to restrict comparative functional studies across Dictyostelia.

To date, more than 150 Dictyostelia species have been described, yet molecular phylogenies indicate that many additional lineages remain undiscovered [6,15]. Dictyostelia species display diverse ecological adaptations and patterns of cell-type differentiation, providing a valuable comparative framework for understanding the evolution of multicellularity and cooperative cell-type specialization. Despite this ecological and phylogenetic diversity, most laboratory research has focused on *D. discoideum*, a Group 4 species characterized by rapid growth, ease of clonal propagation, and comprehensive genomic resources supported by well-established molecular genetics and imaging techniques [16-19]. This experimental tractability has enabled fundamental discoveries in cell motility, chemotaxis, phagocytosis, macropinocytosis, autophagy, and developmental regulation as well as promoted large-scale functional genomics and host-pathogen studies [20-26]. However, the developmental mechanisms of other lineages,

ARTICLE IN PRESS

such as *Heterostelium* (Group2) and members of *Cavenderiaceae* (Group1), remain poorly characterized, partly because efficient genetic manipulation of these non-model species remains technically challenging. Therefore, expanding molecular and genetic analyses to these phylogenetically diverse taxa holds great potential for uncovering new developmental strategies and for deepening our understanding of multicellular complexity across Dictyostelia.

Genetic manipulation in *D. discoideum* has a long history, with gene disruption by homologous recombination established in the 1980s [27]. Over the last several years, plasmid-based CRISPR/Cas9 systems have become the standard approach for genetic manipulation in *D. discoideum*, enabling a wide range of modifications, including knockout, knock-in, and knockdown approaches [18,28-30]. A recent study demonstrated that electroporation of Cas9-single guide RNA (sgRNA) ribonucleoprotein (RNP) complexes enables fluorescent protein knock-in in related Dictyostelia species, thereby advancing genetic engineering in non-model lineages [31]. A major obstacle to genetic manipulation in these species is their non-axenic nature, which leads to degradation of introduced DNA by nucleases associated with bacterial digestion. Additionally, drug-based selection systems are often ineffective, and stable transformation has not yet been achieved in basal species, such as *Acytostelium subglobosum* [32,33]. These characteristics, while reflecting their natural ecology, have made genetic manipulation technically challenging. Therefore, we aimed to extend the CRISPR/Cas9 system developed for *D. discoideum* to phylogenetically diverse dictyostelid lineages, including the early-branching Groups 1 and 2 and the more derived Group 4. A unified genome-editing platform across these lineages would enable meaningful comparative analyses of the conserved and lineage-specific mechanisms underlying multicellularity and cell-type differentiation. To provide biologically interpretable benchmarks for genome editing across Dictyostelia, we targeted two well-characterized developmental genes in *D. discoideum*, *pkaC* and *stlA*. The evolutionary conservation of PkaC across dictyostelids has been well demonstrated by comparative genomic analyses [34], supporting its use as a conserved functional marker across this clade. In addition, StlA, a polyketide synthase required for MPBD biosynthesis in *D. discoideum*, has been reported to be conserved among social amoebae [35]. Consistent with these studies, *pkaC* encodes the catalytic subunit of cAMP-dependent protein kinase A (PKA), a conserved regulator critical for aggregation and multicellular development, whose disruption causes severe aggregation defects [36], *stlA* encodes a polyketide synthase that produces developmental signaling molecules required for proper cAMP-mediated aggregation, with loss-of-function mutants showing delayed aggregation and reduced aggregate size

ARTICLE IN PRESS

[37].Here, we extend CRISPR/Cas9 genome editing beyond *D. discoideum* to multiple Dictyostelia species and demonstrate that donor-oligo co-delivery greatly improves editing efficiency. This platform allows the routine generation of developmental mutants and opens new avenues for comparative studies of multicellular evolution in Dictyostelia.

Results

Targeted knockout of endogenous genes demonstrates functional genome editing in *Polysphondylium violaceum*

In the model organism *D. discoideum*, genome editing via transient expression of CRISPR/Cas9 vectors has been well established [18]. We first tested whether this method could be extended to *P. violaceum*. To this end, the transient expression vector pTM1559 was engineered to include a target sequence from the *stlA* gene and was subsequently introduced into *P. violaceum* cells (Supplementary Fig. 1A). Particularly, high nuclease activity associated with bacterial digestion can hamper DNA introduction in non-axenic strains, and pre-incubation under bacteria-depleted conditions have been suggested to reduce this activity and improve transformation efficiency [38,39]. Using this pretreatment, three independent transformation experiments were conducted. Since *stlA* disruption is known to cause delayed aggregation accompanied by reduced aggregate size during development [37], the putative knockout frequency was initially estimated from the proportion of clones exhibiting this phenotype. This frequency ranged between 0.0% and 29.2%, with putative knockout clones identified in some but not all experiments (Supplementary Fig. 1B). These phenotypic candidates were then further examined using mutation-detection PCR, in which one primer was designed to overlap the predicted Cas9 cleavage site, resulting in inhibited amplification when mutations were introduced at the target locus. Sequence analysis was subsequently performed on four PCR-positive clones, all of which revealed a consistent 2-bp deletion (Supplementary Figs. 1C–D). These results indicate that transient expression of CRISPR/Cas9 can facilitate genome editing in *P. violaceum*; however, the efficiency varied substantially between the experiments.

To enhance the stability of genome editing, we subsequently constructed a CRISPR/Cas9 vector based on a plasmid designed for extrachromosomal expression in *D. discoideum*. This vector contained a Ddp1 replication origin derived from an extrachromosomal plasmid, enabling its amplification within cells (Fig. 1A). Utilizing this backbone, an extrachromosomal CRISPR/Cas9 vector targeting the *stlA* gene was

ARTICLE IN PRESS

generated and introduced into cells (Fig. 1B). Three independent experiments consistently yielded development-defective clones, with frequencies ranging from 13.9% to 27.8% based on phenotypic screening (Fig. 1C). Individual clones were then analyzed by mutation-detection PCR and two of them showed inhibited amplification compared to the wild-type (Fig. 1D). Sequence analysis of the two PCR-positive clones revealed a 3-bp deletion in clone #6 and a 2-bp deletion in clone #8, and both mutants exhibited developmental defects during development (Fig. 1E–F). Typically, a 3-bp deletion is expected to cause only a single amino acid loss and may not cause a substantial functional defect. However, in this case the phenotype manifested, likely because the deletion occurred within the functional ketosynthase family 3 (KS3) domain of StlA, which is evolutionarily conserved between *D. discoideum* and *P. violaceum* (64.3% amino acid identity) [37], and the deleted amino acid corresponds to a conserved residue shared between these species.

Subsequently, we investigated the applicability of this system to another endogenous gene. As a model, we targeted *pkaC*, which encodes the PKA catalytic subunit. Although disruption of *pkaC* has not been characterized in *P. violaceum*, knockout mutants in other Dictyostelia are known to exhibit severe defects in aggregation and subsequent development [36,40], making it a suitable gene for phenotype-based screening. Following introduction of the extrachromosomal CRISPR/Cas9 vector and clonal isolation, approximately 40% of the clones exhibited a development-deficient phenotype (Supplementary Fig. 2A–B). All three sequenced clones carried a 1-bp deletion, and none formed cell aggregation (Supplementary Fig. 2C–D). These results demonstrate that the newly developed extrachromosomal expression vector facilitates the efficient and reproducible isolation of mutant strains in *P. violaceum*.

A potential concern associated with the extrachromosomal expression of CRISPR/Cas9 vectors is the increased risk of off-target effects. However, since extrachromosomal CRISPR/Cas9 vectors generally require more than a week of drug selection to stabilize, short-term selection (such as 4 days) can result in heterogeneous outcomes; in some cells the plasmid is retained, whereas in others it is rapidly lost. This divergence in plasmid retention is an important factor to consider when assessing the potential off-target effects. To investigate this, we cultured CRISPR/Cas9-transformed clones in KK2/HL5 medium containing heat-killed bacteria (HKB), and then reintroduced G418 to evaluate vector retention. Most clones failed to grow under drug selection conditions, with only 2.9% retaining resistance (Supplementary Fig. 2E). These findings indicate that CRISPR clones isolated after a 4-day drug selection

ARTICLE IN PRESS

generally lost drug resistance once the selection pressure was removed. The lack of maintenance of drug resistance not only reduces the likelihood of accumulating off-target mutations but also offers an experimental advantage by permitting the reuse of a similar expression vector for functional rescue experiments or heterologous protein expression without interference.

CRISPR/Cas9-mediated gene disruption in Group 1 and Group 2 species

To assess the applicability of the constitutive CRISPR/Cas9 system across diverse dictyostelid lineages, we subsequently evaluated its functionality in representative species from Groups 1 and 2. Since the vector contains expression elements derived from *D. discoideum* known as Group 4, its activity in more distantly related taxa could not be assumed, making such tests essential for determining the broad utility of this method. As a representative of Group 2, *Heterostelium pallidum* (formerly *Polysphondylium pallidum*) was targeted at the *pkaC* gene (Fig. 2A), disruption of which results in a development-deficient phenotype [40]. Among the three independent transformations, only one clone exhibited the expected phenotype (Fig. 2B). Mutation-detection PCR using a newly designed primer extending one nucleotide beyond the predicted Cas9 cleavage site showed the absence of a wild-type band, confirming the presence of an indel mutation in the target region (Fig. 2C and Supplementary Fig. 3). Because conventional mutation-detection PCR strategies were originally developed for *D. discoideum* [18], their sensitivity may be reduced in more distantly related dictyostelids, occasionally resulting in false-positive amplification when primers that fully span the target sequence are used (Supplementary Fig. 3). Genome sequencing confirmed a 7-bp deletion at the target site (Fig. 2D), and this clone demonstrated the development-defective phenotype (Fig. 2E).

We next examined *Cavenderia fasciculata* (formerly *Dictyostelium fasciculatum*), a Group 1 species for which gene disruption via homologous recombination has not been previously reported. Transformation with the extrachromosomal CRISPR vector targeting *pkaC* resulted in a substantially higher putative knockout frequency, averaging 29.1% (Fig. 3A–B). Mutation-detection PCR confirmed gene disruption, and sequencing analysis of the six clones identified mutations at the target site in all instances (Fig. 3C–D). All the analyzed clones exhibited an aggregation-defective phenotype (Fig. 3E). Together, these findings demonstrate that the extrachromosomal CRISPR/Cas9 vector is effective not only in Group 4 but also in Groups 1 and 2. Although *C. fasciculata* exhibited high editing efficiency, *H. pallidum* produced infrequent mutants, suggesting that additional

ARTICLE IN PRESS

optimization is necessary to achieve robust gene editing in this species.

Cross-species complementation of PkaC function using *D. discoideum* sequence

Having established efficient CRISPR/Cas9-mediated gene disruption across multiple Dictyostelia species, we subsequently evaluated the advantages of this approach over conventional homologous recombination. A primary advantage of the CRISPR-based approach is that the resulting knockout strains are marker-free, allowing successive genetic manipulations without the need for a marker recycling step. Contrastingly, homologous recombination-based gene disruption requires the selection marker to be removed before additional genetic modifications, often using Cre-mediated excision. Identifying marker-free clones typically requires screening large numbers of isolates, making multiple knockouts or complementation assays laborious and time-consuming [13].

To take advantage of the marker-free nature of the CRISPR-based system, we tested whether overexpression of the *D. discoideum* ortholog could restore aspects of PkaC function in knockout strains of *H. pallidum* and *C. fasciculata*. In *D. discoideum*, overexpression of *pkaC* driven by the *act15* promoter in *pkaC*-null mutants restores aggregation but does not support progression beyond the slug stage, resulting in defective culmination [41]. This indicates that its functional rescue is limited to early developmental stages. Given this limited rescue in *D. discoideum*, we next examined whether similar early-stage functions could be recovered in other Dictyostelia. After confirming that the knockout strains were marker-free, as indicated by their G418 sensitivity, *D. discoideum pkaC* was introduced using an overexpression vector driven by the *act15* promoter. In both species, expression of *D. discoideum pkaC* effectively restored early developmental processes, including formation of aggregation centers (Figs. 2E & 3E). However, the complemented strains did not regain their ability to undergo normal fruiting body morphogenesis, which remained incomplete in both *H. pallidum* and *C. fasciculata* (Supplementary Fig. 4). These findings indicate that although *D. discoideum pkaC* can restore conserved early functions such as aggregation, it cannot replace the species-specific spatial and temporal regulation of PKA required for proper culmination.

Collectively, these findings highlight that CRISPR-derived knockout strains are marker-free and enable rapid cross-species functional testing using expression vectors. This approach provides a powerful platform for comparative analyses of orthologous gene functions, allowing the dissection of conserved roles and lineage-specific regulatory divergence across Dictyostelia.

ARTICLE IN PRESS

Donor oligo-mediated enhancement of CRISPR/Cas9 genome editing in Dictyostelia

Previous analyses indicated that gene disruption efficiency in *H. pallidum* remained low, thus improving editing efficiency is an important challenge. In this context, van Gestel and colleagues recently described a genome editing approach involving the delivery of an RNP complex, comprising *Streptococcus pyogenes* Cas9 (SpCas9), crRNA, and tracrRNA, into cells alongside a donor oligo [31]. Notably, they demonstrated that supplying a donor oligo at a relatively high concentration (2.4 μM) significantly increased the disruption efficiency of a fluorescent protein previously knocked into the *D. discoideum* genome.

To evaluate whether donor oligos could enhance the disruption of endogenous genes in *D. discoideum*, we targeted the *pkaC* gene using a transient CRISPR/Cas9 vector while simultaneously introducing a donor oligo. In this experiment, clones exhibiting aggregation defects were classified as gene disruption mutants. The donor oligo was designed following the strategy previously described for RNP-mediated CRISPR/Cas9 gene disruption in *D. discoideum* [31], with short homology arms positioned relative to the Cas9 cleavage site to enable efficient editing and PCR-based validation. It consisted of a 5′ homology arm of 28 bp including four bases upstream of the PAM, and a 3′ homology arm of 28 bp starting five bases upstream of the PAM, flanking a 37 bp insertion comprising an HA tag sequence and a stop codon. This design allowed straightforward verification of the edited alleles using mutation-detection PCR (Fig. 4A). A comparison between conditions with and without the donor oligo revealed that, on average, 50.9% of clones displayed the aggregation-defective phenotype in the absence of the donor, whereas this proportion increased to 84.3% in its presence (Fig. 4B). From each condition, four clones were selected, and PCR amplification spanning the donor tag region and the downstream *pkaC* sequence yielded products only from clones obtained with the donor oligo, indicating successful donor integration (Fig. 4C). Subsequent sequence analysis confirmed the insertion of the complete 37 bp sequence at the target locus, thereby disrupting the gene (Fig. 4D).

Given that donor oligos increased the frequency of gene disruption, we subsequently investigated whether gene disruption mutants could be obtained without drug selection by cloning cells after 1 day of recovery following electroporation. Even under selection-free conditions, the average frequency of aggregation-defective clones reached 11.0%, whereas addition of donor oligos further increased this frequency to 28.6% (Supplementary Fig. 5). These findings indicate that the co-introduction of donor

ARTICLE IN PRESS

oligos with CRISPR vectors facilitates the isolation of gene disruption mutants with a sufficiently high efficiency even under selection-free conditions.

Finally, we applied this methodology to *H. pallidum*, a species known for its low genome-editing efficiency. Under conventional conditions without donor oligos, only one disruption mutant was identified out of 108 analyzed clones (36 clones per trial, three independent trials), indicating that gene disruption was rarely achieved. Contrastingly, when donor oligos were co-electroporated with the extrachromosomal CRISPR/Cas9 vector and cells were subjected to 4 days of drug selection, disruption mutants were obtained in two out of three trials, each yielding several independent clones, resulting in a marked overall increase in efficiency (Fig. 5). Extending the drug selection period from 4 to 6 days further improved the efficiency of donor oligo-mediated disruption, increasing the average mutation frequency from 8.3% to 20.4% (Supplementary Fig. 6). These findings indicate that the simultaneous introduction of donor oligos improves gene disruption efficiency and offers a valuable strategy for genome editing in Dictyostelia species where conventional methods are insufficient.

ARTICLE IN PRESS

Discussion

This study establishes a broadly applicable plasmid-based CRISPR/Cas9 system for genome editing across multiple dictyostelid lineages. A summary of the genome-editing protocols tested for each dictyostelid species and their resulting efficiencies is provided in Supplementary Table S1. Recent work has also shown that Cas9-sgRNA delivery is feasible in non-*D. discoideum* species, offering a vector-independent method for introducing CRISPR/Cas9 activity [31]. In contrast, plasmid-based expression provides practical advantages, as Cas9 and sgRNA are generated intracellularly without purification of Cas9 protein or RNA components. This reduces both the technical burden and cost of genome-editing experiments, while also yielding higher and more consistent editing efficiencies in several contexts. For example, in cells carrying a fluorescent protein knock-in, RNP-mediated gene disruption achieves only approximately 5% efficiency without donor DNA [31], whereas transiently selected plasmid-based CRISPR/Cas9 editing using conventional SpCas9 can achieve efficiencies >97% under similar conditions [42]. When the same target, *pkaC*, was edited in *D. discoideum* using this plasmid-based system, three independent experiments yielded mutation frequencies averaging 28.6% under selection-free conditions. In comparison, *pkaC* editing using Cas9-sgRNA RNPs with donor oligos achieved

ARTICLE IN PRESS

substantially lower efficiencies, averaging approximately 9% in a previous work [31]. Although direct comparison is complicated by differences in gRNA position, the plasmid-based method appears to achieve higher and more consistent efficiencies, likely due to appropriate Cas9/sgRNA expression. Moreover, plasmid systems readily accommodate Cas9 derivatives such as nickase and dCas9 [28,29], providing a flexible platform for applications including base editing, transcriptional modulation, and chromatin targeting [43]. Collectively, RNP- and plasmid-based systems provide complementary tools for dictyostelid genome engineering, enabling researchers to select the most suitable approach depending on experimental goals, available resources, and required precision.

The CRISPR/Cas9 plasmid used in this study was originally developed for *D. discoideum* and contains both Cas9 and sgRNA expression cassettes in a single vector [18]. Cas9 expression is driven by the *act15* promoter, whereas sgRNA transcription is controlled by an isoleucine tRNA promoter. The tRNA-sgRNA fusion transcript is naturally cleaved by the conserved tRNA processing machinery, RNase P and RNase Z, to generate mature sgRNAs [18,44]. Although the vector relies on the *D. discoideum* transcriptional system, previous studies have shown that actin-based promoters from *D. discoideum* function effectively in other Dictyostelia [13]. Consistently, the isoleucine tRNA sequence used in this study was conserved in *H. pallidum* and *P. violaceum*. In *C. fasciculata*, the primary tRNA sequence is less conserved; however, tRNA processing depends mainly on structural rather than sequence features, and efficient gene disruption observed in this species suggests that sgRNA maturation occurs properly. These results indicated that *D. discoideum*-derived expression systems are broadly functional across Dictyostelia, providing a practical foundation for cross-species genome editing.

Although CRISPR/Cas9 provides a powerful approach for targeted mutagenesis, potential off-target effects remain a concern. When complete genomic information is available, potential off-target sites can be computationally predicted, allowing the design of guide RNAs with minimal similarity to other loci [45,46]. However, many non-model Dictyostelia species still possess fragmented or incompletely annotated genomes, indicating that Cas9 may interact with unrecognized homologous sequences. Thus, the risk of off-target mutations is likely higher in these species than in *D. discoideum*. In this study, we analyzed multiple independent mutant clones, and the reproducibility of their developmental phenotypes indicated that the observed defects most likely reflected disruption of the intended target rather than random off-target events. In *D. discoideum*, even sequences differing by only a single mismatch (19/20 bp identity) show off-target editing frequencies as low as 0.6% after 4 days of transient

ARTICLE IN PRESS

selection [26], suggesting that the conditions and guide design strategy employed here are effective at minimizing unintended cleavage. In comparison to the notably low GC content of the *D. discoideum* genome, the other dictyostelids examined here exhibited relatively higher GC content, on the order of approximately 10% [14], which is expected to facilitate the design of higher specific guide RNAs. Nevertheless, species with higher genomic GC content did not demonstrate superior editing efficiencies compared with *D. discoideum*, and no definitive correlation was identified between genome GC content and editing efficiency. These findings suggested that increased GC content does not inherently result in enhanced editing efficiency under the conditions employed. Additional safeguards are available for applications requiring even greater editing precision. The Cas9 nickase system [28] provides a high-specificity alternative using paired guides. Moreover, since the CRISPR-derived knockout strains generated in this study are marker-free, the targeted gene can be reintroduced driven by its endogenous promoter, enabling rescue experiments that better reflect its native regulatory context and support the direct confirmation of on-target gene disruption.

Genetic transformation of non-model Dictyostelia remains technically challenging owing to its non-axenic growth and high nuclease activity associated with bacterial digestion. In this study, we tested several electroporation conditions but did not observe marked improvement under the parameters examined. These results suggest that transformation efficiency may depend on species-specific cellular properties and could require tailored optimization. Contrastingly, pre-incubation under bacteria-depleted conditions prior to electroporation proved to be critical for successful transformation. However, prolonged starvation caused cells to elongate and reduced transformation efficiency, indicating that the timing of pre-starvation requires careful control. While *D. discoideum* allowed selection-free knockout generation with co-introduction of donor oligos, applying short-term drug selection substantially increased the mutation frequency in both *D. discoideum* and *H. pallidum*. Moreover, extending the G418 selection period from 4 to 6 days enhanced the mutation efficiency in *H. pallidum*. These results indicate that a brief or partial selection period is advantageous compared with a completely selection-free protocol. Newly developed methods are also directly applicable to non-axenic strains such as NC4 in *D. discoideum*, which retain wild-type feeding behavior. In axenic derivatives, constitutive activation of the Ras-PI3K pathway leads to persistent PIP3 signaling and excessive macropinocytosis, creating serious confounding effects on studies of chemotaxis and other signaling processes [47,48]. Therefore, genome editing in NC4 cells and other non-axenic backgrounds will be particularly valuable for investigating cellular behavior

ARTICLE IN PRESS

under more physiological conditions. A further practical consideration is the limited applicability of drug-selection markers across Dictyostelia. Some species, such as *A. subglobosum*, are resistant to commonly used antibiotics [33], and even *D. discoideum* becomes less sensitive to blasticidin when co-cultured with bacteria [17,31]. In such cases, RNP-based or plasmid-based selection-free strategies combined with donor oligos provide workable alternatives for obtaining mutants. The continued development of species-specific transformation protocols and promoter systems is essential to expand genome-editing applications across diverse Dictyostelia lineages.

The incomplete rescue by *D. discoideum* PkaC is consistent with previous findings in *D. discoideum*, where *act15*-driven overexpression restored aggregation but disrupts subsequent morphogenesis [41]. These observations demonstrate that the precise temporal and spatial regulation of PKA activity is essential for the transition from aggregation to culmination. In our cross-species assays, constitutive expression likely bypassed these regulatory controls, leading to defective morphogenesis even when early-stage functions were recovered. Consistent with this view, the expression of *H. pallidum pkaC* under its endogenous promoter fully restored development [40], reinforcing the importance of properly timed activation of the cAMP-PKA pathway. Structural divergence between orthologs may further contribute to incomplete rescue. While the catalytic domain is relatively well conserved, the C-terminal regulatory region and lineage-specific N-terminal sequences show substantial divergence and may be involved in interactions with regulatory subunits or upstream activators. These differences could limit full functional compatibility across species. Collectively, these observations suggest that while the core PKA signaling logic is conserved, enabling partial rescue of early developmental processes, both regulatory dynamics and protein-level divergence have been evolutionarily rewired among dictyostelid lineages.

The CRISPR/Cas9-based system established here thus provides a robust genetic platform for comparative evolutionary studies in Dictyostelia, enabling direct experimental testing of signaling pathways that originate in unicellular contexts for multicellular development. This framework will facilitate future mechanistic dissections of regulatory innovations that underlie the evolution of multicellularity.

Methods

Vector constructions

The CRISPR/Cas9 expression vectors used in this study were derived from previously established plasmids, including pTM1599, which was described in a previous study [42].

ARTICLE IN PRESS

A new vector, pTM1660, was constructed by excising the Cas9 gene, sgRNA cassette, and drug-resistance marker from pTM1644 [42] and inserting these elements into the constitutive expression vector pDM304 [49]. Both pTM1599 and pTM1660 contained Cas9, sgRNA, and a drug resistance cassette on a single plasmid backbone, enabling all-in-one expression. Target-specific guide RNAs were introduced into these vectors by Golden Gate assembly using BpiI for pTM1599 and Esp3I for pTM1660 [29]. Because web-based CRISPR design tools for *D. discoideum* were not applicable to other dictyostelid species, sgRNAs were designed using genome sequences obtained from NCBI. These sequences were used to build a local database for Cas-Designer and Cas-OFFinder (Binary ver. 2.4) to predict on- and off-target sites [50]. Guide RNAs were designed to target *stlA* (KAF2071723.1) and *pkaC* (KAF2074596.1) in *P. violaceum*, *pkaC* (XP_020433934.1) in *H. pallidum*, and *pkaC* (XP_004362292.1) in *C. fasciculata*. A full-length *stlA* sequence assembled from two contigs (KAF2071723.1 and KAF2070697.1) has been reported previously [37]. To ensure target specificity, candidate guide RNAs were filtered based on the Cas-Designer output to retain only target sites corresponding to a single unique genomic locus (mismatch number "1,0,0"). Thus, the selected *pkaC* and *stlA* target sites did not have duplicated copies at the sequence level in the examined dictyostelids. The sequences of designed guide RNAs are provided in Supplementary Table S2, and the list of CRISPR/Cas9 vectors containing each guide RNA is shown in Supplementary Table S3. For complementation, the full-length *D. discoideum pkaC* sequence was amplified by PCR and cloned into the *D. discoideum* expression vector pTX-GFP to generate plasmid pTM2439.

Cell culture and development

D. discoideum AX2 and its transformants were cultured in HL5 medium at 22°C or on SM agar plates with *Klebsiella pneumoniae* (KpGe). *P. violaceum* (QSvi11, NBRP-ID: S90889), *H. pallidum* (PN500, NBRP-ID: S00222), and *C. fasciculata* (SH3, NBRP-ID: S00492) were obtained from the NBRP collection. *C. fasciculata* was grown on 5×LP agar plates with KpGe, whereas *P. violaceum* and *H. pallidum* were maintained on 1/5 SM agar plates with KpGe. For clone isolation, transformants were plated on species-specific agar plates with KpGe: SM for *D. discoideum*, 1/5 SM for *P. violaceum* and *H. pallidum*, and 5×LP for *C. fasciculata*. For drug selection, transformants were transferred to liquid medium to allow uniform exposure to antibiotics. Heat-killed *K. pneumoniae* (HKB) was supplied as a nutrient source. Cells were grown in 90% KK2 buffer supplemented with 10% HL5 medium at 22°C, which supported better proliferation than KK2/HKB alone [51].

Cells grown with KpGe on species-specific agar were collected during the

ARTICLE IN PRESS

vegetative phase, washed three times with KK2 buffer, and resuspended in 3.0×10^6 cells/mL. A 1-mL suspension (~3×10^5 cells/cm^2) was plated onto 1.5% non-nutrient KK2 agar in 35-mm dishes. After a 20-min settling period, excess KK2 was removed, and plates were incubated at 22°C under ambient light to induce development.

Transformation

Transformation of *D. discoideum* was performed as described previously [29] with minor modifications. To introduce donor oligos, 2.4 µL of 100 µM oligos (Supplementary Table S4) were added to 100 µL of cells immediately before electroporation. After pulsing, the cells were transferred into 10 mL of HL5 medium. To achieve transient expression of Cas9 and sgRNA, 10 µg/mL G418 was added 8–16 h after electroporation. For selection-free experiments, the cells were mixed with KpGe without antibiotic addition and cloned on SM agar plates. Transformation of *P. violaceum*, *H. pallidum*, and *C. fasciculata* was conducted following the same basic procedure with species-specific adjustments. Before electroporation, cells were washed three times with KK2 to remove KpGe, then incubated in KK2 for 5 h under bacteria-depleted conditions, thereby reducing nuclease activity produced by cells for bacterial digestion. Cells were resuspended at 1.0×10^8 cells/mL in H50 buffer, and 1.0×10^7 cells were used for each electroporation. Electroporation was performed using two pulses separately by 5 s at 25 µF. The field strength was 0.65 kV for *P. violaceum* and 0.55 kV for *H. pallidum* and *C. fasciculata*. After electroporation, the cells were incubated on ice for 5 min, then transferred to a medium containing 1 mL HL5, 9 mL KK2, and 200 µL HKB. To isolate transformants under extrachromosomal expression vector, G418 was added 8–16 h post-electroporation at species-specific concentrations, 10 µg/mL for *P. violaceum*, 100 µg/mL for *H. pallidum*, and 20 µg/mL for *C. fasciculata*, followed by 4 days of incubation. The cells were then mixed with KpGe and plated on species-appropriate agar (1/5 SM for *P. violaceum* and *H. pallidum*, 5×LP for *C. fasciculata*) for clone isolation.

Phenotypic and genotypic analysis of transformants

To screen transformants for development-defective phenotypes, clones were plated onto 1/5 SM or 5×LP medium in 12-well plates or 10-cm dishes covered with a bacterial lawn of KpGe. Plates were incubated at 22°C, and the formation and progression of multicellular aggregates were observed. Clones exhibiting delayed or absent aggregation were classified as development-defective mutants. For genomic DNA extraction, cells from each colony were suspended in ProK solution (0.5× Taq buffer, 0.5% NP-40, 50 ng/µL Proteinase K) and incubated at 56°C for 45 min followed by 95°C for 10 min. The resulting lysates were used as PCR templates. The target regions

ARTICLE IN PRESS

were amplified using Ex Premier DNA Polymerase (TaKaRa) under optimized PCR conditions for each species. Mutation-detection PCR was designed differently for transformants with and without donor oligo insertion. For all gel electrophoresis images shown in the main and supplementary figures, uncropped, full-length gel images are provided in Supplementary Figure 7, with the cropped regions indicated by dashed boxes. For transformants generated without donor oligos, primers flanking the Cas9 cleavage site were used such that wild-type alleles produced a PCR product, whereas disrupted alleles did not (Supplementary Fig. 3). For donor-oligo–mediated knockouts, primers annealing within the HA tag sequence allowed specific amplification only when the donor sequence was correctly inserted. The primer sequences used for mutation detection are listed in Supplementary Table S2.

ARTICLE IN PRESS

ARTICLE IN PRESS

References

1 Hillmann, F. *et al.* Multiple Roots of Fruiting Body Formation in Amoebozoa. *Genome Biol Evol* **10**, 591–606, doi:10.1093/gbe/evy011 (2018).

2 Kawabe, Y., Du, Q., Schilde, C. & Schaap, P. Evolution of multicellularity in Dictyostelia. *Int J Dev Biol* **63**, 359–369, doi:10.1387/ijdb.190108ps (2019).

3 Medina, J. M., Shreenidhi, P. M., Larsen, T. J., Queller, D. C. & Strassmann, J. E. Cooperation and conflict in the social amoeba Dictyostelium discoideum. *Int J Dev Biol* **63**, 371–382, doi:10.1387/ijdb.190158jm (2019).

4 Shirokawa, Y., Shimada, M., Shimada, N. & Sawai, S. Prestalk-like positioning of de-differentiated cells in the social amoeba Dictyostelium discoideum. *Sci Rep* **14**, 7677, doi:10.1038/s41598-024-58277-3 (2024).

5 Schaap, P. *et al.* Molecular phylogeny and evolution of morphology in the social amoebas. *Science* **314**, 661–663, doi:10.1126/science.1130670 (2006).

6 Sheikh, S. *et al.* A New Classification of the Dictyostelids. *Protist* **169**, 1–28, doi:10.1016/j.protis.2017.11.001 (2018).

7 Singh, R., Schilde, C. & Schaap, P. A core phylogeny of Dictyostelia inferred from genomes representative of the eight major and minor taxonomic divisions of the group. *BMC Evol Biol* **16**, 251, doi:10.1186/s12862-016-0825-7 (2016).

8 Glockner, G. & Heidel, A. J. Centromere sequence and dynamics in Dictyostelium discoideum. *Nucleic Acids Res* **37**, 1809–1816, doi:10.1093/nar/gkp017 (2009).

9 Heidel, A. J. *et al.* Phylogeny-wide analysis of social amoeba genomes highlights ancient origins for complex intercellular communication. *Genome Res* **21**, 1882–1891, doi:10.1101/gr.121137.111 (2011).

10 Kin, K., Forbes, G., Cassidy, A. & Schaap, P. Cell-type specific RNA-Seq reveals novel roles and regulatory programs for terminally differentiated Dictyostelium cells. *BMC Genomics* **19**, 764, doi:10.1186/s12864-018-5146-3 (2018).

11 Parikh, A. *et al.* Conserved developmental transcriptomes in evolutionarily divergent species. *Genome Biol* **11**, R35, doi:10.1186/gb-2010-11-3-r35 (2010).

12 Kin, K., Chen, Z. H., Forbes, G. & Schaap, P. Evolution of a novel cell type in Dictyostelia required gene duplication of a cudA-like transcription factor. *Curr Biol* **32**, 428–437 e424, doi:10.1016/j.cub.2021.11.047 (2022).

13 Kawabe, Y. *et al.* Activated cAMP receptors switch encystation into sporulation. *Proc Natl Acad Sci U S A* **106**, 7089–7094, doi:10.1073/pnas.0901617106 (2009).

14 Narita, T. B. *et al.* Loss of the Polyketide Synthase StlB Results in Stalk Cell Overproduction in Polysphondylium violaceum. *Genome Biol Evol* **12**, 674–683, doi:10.1093/gbe/evaa079 (2020).

15 Baldauf, S. L., Romeralo, M., Fiz-Palacios, O. & Heidari, N. A Deep Hidden Diversity of Dictyostelia. *Protist* **169**, 64–78, doi:10.1016/j.protis.2017.12.005 (2018).

ARTICLE IN PRESS

ARTICLE IN PRESS

16 Hashimura, H. *et al.* Multi-color fluorescence live-cell imaging in Dictyostelium discoideum. *Cell Struct Funct* **49**, 135–153, doi:10.1247/csf.24065 (2024).

17 Paschke, P. *et al.* Rapid and efficient genetic engineering of both wild type and axenic strains of Dictyostelium discoideum. *PLoS One* **13**, e0196809, doi:10.1371/journal.pone.0196809 (2018).

18 Sekine, R., Kawata, T. & Muramoto, T. CRISPR/Cas9 mediated targeting of multiple genes in Dictyostelium. *Sci Rep* **8**, 8471, doi:10.1038/s41598-018-26756-z (2018).

19 Yamashita, K., Shimane, K. & Muramoto, T. Optogenetic control of cAMP oscillations reveals frequency-selective transcription factor dynamics in Dictyostelium. *Development* **152**, dev204403, doi:10.1242/dev.204403 (2025).

20 Mesquita, A. *et al.* Autophagy in Dictyostelium: Mechanisms, regulation and disease in a simple biomedical model. *Autophagy* **13**, 24–40, doi:10.1080/15548627.2016.1226737 (2017).

21 Gruenheit, N. *et al.* Mutant resources for functional genomics in Dictyostelium discoideum using REMI-seq technology. *BMC Biol* **19**, 172, doi:10.1186/s12915-021-01108-y (2021).

22 Huber, R. J., Steimle, P. A. & Damer, C. K. Cell biology of Dictyostelium. *BMC Mol Cell Biol* **26**, 25, doi:10.1186/s12860-025-00550-y (2025).

23 Storey, C. L., Williams, R. S. B., Fisher, P. R. & Annesley, S. J. Dictyostelium discoideum: A Model System for Neurological Disorders. *Cells* **11**, doi:10.3390/cells11030463 (2022).

24 Williams, R. S. B. *et al.* Moving the Research Forward: The Best of British Biology Using the Tractable Model System Dictyostelium discoideum. *Cells* **10**, doi:10.3390/cells10113036 (2021).

25 Hao, Y. *et al.* A transcription factor complex in Dictyostelium enables adaptive changes in macropinocytosis during the growth-to-development transition. *Dev Cell* **59**, 645–660 e648, doi:10.1016/j.devcel.2024.01.012 (2024).

26 Ogasawara, T. *et al.* CRISPR/Cas9-based genome-wide screening of Dictyostelium. *Sci Rep* **12**, 11215, doi:10.1038/s41598-022-15500-3 (2022).

27 De Lozanne, A. & Spudich, J. A. Disruption of the Dictyostelium myosin heavy chain gene by homologous recombination. *Science* **236**, 1086–1091, doi:10.1126/science.3576222 (1987).

28 Iriki, H., Kawata, T. & Muramoto, T. Generation of deletions and precise point mutations in Dictyostelium discoideum using the CRISPR nickase. *PLoS One* **14**, e0224128, doi:10.1371/journal.pone.0224128 (2019).

29 Yamashita, K., Iriki, H., Kamimura, Y. & Muramoto, T. CRISPR Toolbox for Genome Editing in Dictyostelium. *Front Cell Dev Biol* **9**, 721630, doi:10.3389/fcell.2021.721630 (2021).

30 Yamashita, K. & Muramoto, T. Efficient endogenous protein labelling in Dictyostelium using CRISPR/Cas9 knock-in and split fluorescent proteins. *PLoS One* **20**, e0326577, doi:10.1371/journal.pone.0326577 (2025).

31 Garriga-Canut, M. *et al.* Unlocking CRISPR-Cas9 editing for widely diverse Dictyostelid species. *Mol Syst Biol*, doi:10.1038/s44320-025-00180-8 (2026).

ARTICLE IN PRESS

ARTICLE IN PRESS

32 Kuwayama, H., Tohyama, T. & Urushihara, H. Cross-species functional complementation of cellulose synthase during the development of cellular slime molds. *Dev Growth Differ* **56**, 526–533, doi:10.1111/dgd.12153 (2014).

33 Mohri, K., Kiyota, Y., Kuwayama, H. & Urushihara, H. Temporal and non-permanent division of labor during sorocarp formation in the social amoeba Acytostelium subglobosum. *Dev Biol* **375**, 202–209, doi:10.1016/j.ydbio.2013.01.003 (2013).

34 Kin, K. *et al.* The protein kinases of Dictyostelia and their incorporation into a signalome. *Cell Signal* **108**, 110714, doi:10.1016/j.cellsig.2023.110714 (2023).

35 Glockner, G. *et al.* The multicellularity genes of dictyostelid social amoebas. *Nat Commun* **7**, 12085, doi:10.1038/ncomms12085 (2016).

36 Mann, S. K. & Firtel, R. A. A developmentally regulated, putative serine/threonine protein kinase is essential for development in Dictyostelium. *Mech Dev* **35**, 89–101, doi:10.1016/0925-4773(91)90060-j (1991).

37 Yamasaki, D. T., Araki, T. & Narita, T. B. The polyketide synthase StlA is involved in inducing aggregation in Polysphondylium violaceum. *Biosci Biotechnol Biochem* **86**, 1590–1598, doi:10.1093/bbb/zbac144 (2022).

38 Kawabe, Y., Enomoto, T., Morio, T., Urushihara, H. & Tanaka, Y. LbrA, a protein predicted to have a role in vesicle trafficking, is necessary for normal morphogenesis in Polysphondylium pallidum. *Gene* **239**, 75–79, doi:10.1016/s0378-1119(99)00379-0 (1999).

39 Muramoto, T., Takeda, S., Furuya, Y. & Urushihara, H. Reverse genetic analyses of gamete-enriched genes revealed a novel regulator of the cAMP signaling pathway in Dictyostelium discoideum. *Mech Dev* **122**, 733–743, doi:10.1016/j.mod.2004.11.015 (2005).

40 Kawabe, Y., Schilde, C., Du, Q. & Schaap, P. A conserved signalling pathway for amoebozoan encystation that was co-opted for multicellular development. *Sci Rep* **5**, 9644, doi:10.1038/srep09644 (2015).

41 Mann, S. K., Yonemoto, W. M., Taylor, S. S. & Firtel, R. A. DdPK3, which plays essential roles during Dictyostelium development, encodes the catalytic subunit of cAMP-dependent protein kinase. *Proc Natl Acad Sci U S A* **89**, 10701–10705, doi:10.1073/pnas.89.22.10701 (1992).

42 Asano, Y. *et al.* Knock-in and precise nucleotide substitution using near-PAMless engineered Cas9 variants in Dictyostelium discoideum. *Sci Rep* **11**, 11163, doi:10.1038/s41598-021-89546-0 (2021).

43 Wang, H., La Russa, M. & Qi, L. S. CRISPR/Cas9 in Genome Editing and Beyond. *Annu Rev Biochem* **85**, 227–264, doi:10.1146/annurev-biochem-060815-014607 (2016).

44 Muramoto, T., Iriki, H., Watanabe, J. & Kawata, T. Recent Advances in CRISPR/Cas9-Mediated Genome Editing in Dictyostelium. *Cells* **8**, doi:10.3390/cells8010046 (2019).

45 Hsu, P. D. *et al.* DNA targeting specificity of RNA-guided Cas9 nucleases. *Nat Biotechnol* **31**, 827–832, doi:10.1038/nbt.2647 (2013).

46 Pattanayak, V. *et al.* High-throughput profiling of off-target DNA cleavage reveals RNA-programmed Cas9

ARTICLE IN PRESS

ARTICLE IN PRESS

nuclease specificity. *Nat Biotechnol* **31**, 839–843, doi:10.1038/nbt.2673 (2013).

47 Nichols, J. M., Veltman, D. & Kay, R. R. Chemotaxis of a model organism: progress with Dictyostelium. *Curr Opin Cell Biol* **36**, 7–12, doi:10.1016/j.ceb.2015.06.005 (2015).

48 Veltman, D. M. *et al.* A plasma membrane template for macropinocytic cups. *Elife* **5**, doi:10.7554/eLife.20085 (2016).

49 Veltman, D. M., Akar, G., Bosgraaf, L. & Van Haastert, P. J. A new set of small, extrachromosomal expression vectors for Dictyostelium discoideum. *Plasmid* **61**, 110–118, doi:10.1016/j.plasmid.2008.11.003 (2009).

50 Park, J., Bae, S. & Kim, J. S. Cas-Designer: a web-based tool for choice of CRISPR-Cas9 target sites. *Bioinformatics* **31**, 4014–4016, doi:10.1093/bioinformatics/btv537 (2015).

51 Kawabe, Y. & Schaap, P. Development of the dictyostelid Polysphondylium violaceum does not require secreted cAMP. *Biol Open* **12**, doi:10.1242/bio.059728 (2023).

ARTICLE IN PRESS

ARTICLE IN PRESS

Acknowledgements

We thank Dr. Takaaki B. Narita for valuable advice on the *stlA* gene of *P. violaceum*, and are grateful to Mr. Yuichiro Ishiyama, Mr. Takanori Ogasawara, and Ms. Mio Ito for their assistance with cloning parts of the CRISPR/Cas9 vectors. We also acknowledge the National BioResource Project (NBRP) Nenkin for supplying the dictyostelid species used in this work. Paperpal and ChatGPT were used solely to improve the English language during the revision process.

Author contributions

S.O. performed most of the experiments. S.D. and T.S. optimized CRISPR/Cas9 conditions in non-model Dictyostelia. K.Y. and Y.Y. contributed to improving cell culture and selection procedures. T.M. conceived and designed the study, and supervised the project. T.M. wrote the manuscript with contributions from K.Y. and S.O. All authors discussed the results and agreed to the published version of the manuscript.

ARTICLE IN PRESS

Funding

This work was supported by the Japan Society for the Promotion of Science (JSPS) KAKENHI (23K05785 to T.M.) and by a JSPS Research Fellowship for Young Scientists (DC1; 23KJ1977 to K.Y.).

Data availability statement

All data are presented in the manuscript or the supplementary materials. The plasmids and cell lines generated in this study are available from NBRP Nenkin.

Additional Information

Competing interests

The authors declare no competing interests.

ARTICLE IN PRESS

Figure legends

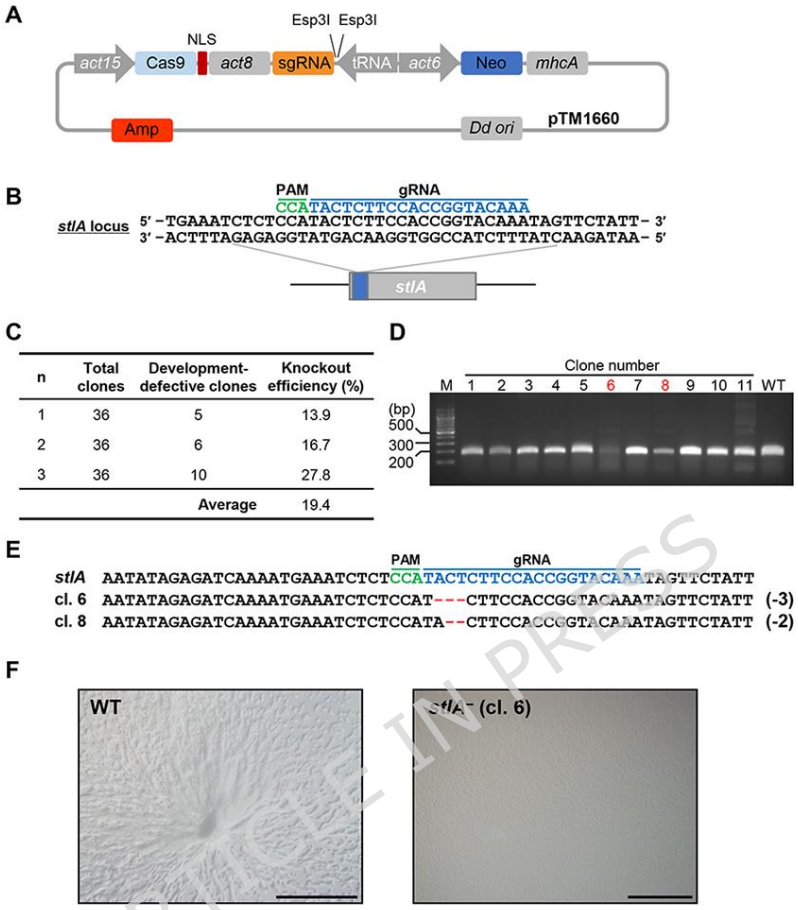

Figure 1. Knockout of *stlA* using a newly developed extrachromosomal CRISPR vector in *P. violaceum*.

(A) Schematic diagram of the Cas9 all-in-one vector (pTM1660) used for constitutive expression. (B) Schematic representation of the *stlA* target region. The ketosynthase (KS) domain is indicated by the blue box. (C) Phenotypic screening for development-defective clones. Among 36 clones analyzed per experiment, those exhibiting development defects were counted to calculate putative knockout frequency. (D) Mutation detection PCR of a randomly selected subset of 11 clones. Clones highlighted in red represent candidates selected for sequencing. (E) Sequence analysis of the genomic region containing the target site. The target sequence is shown in blue, the PAM sequence in green, and mutations in red. Numbers in parentheses indicate the size of the mutation. (F) Developmental phenotypes of wild-type and mutant strains at 7 h after starvation. Wild-type cells formed aggregation centers, whereas cl. 6 mutant showed aggregation defect. Scale bars: 0.5 mm.

ARTICLE IN PRESS

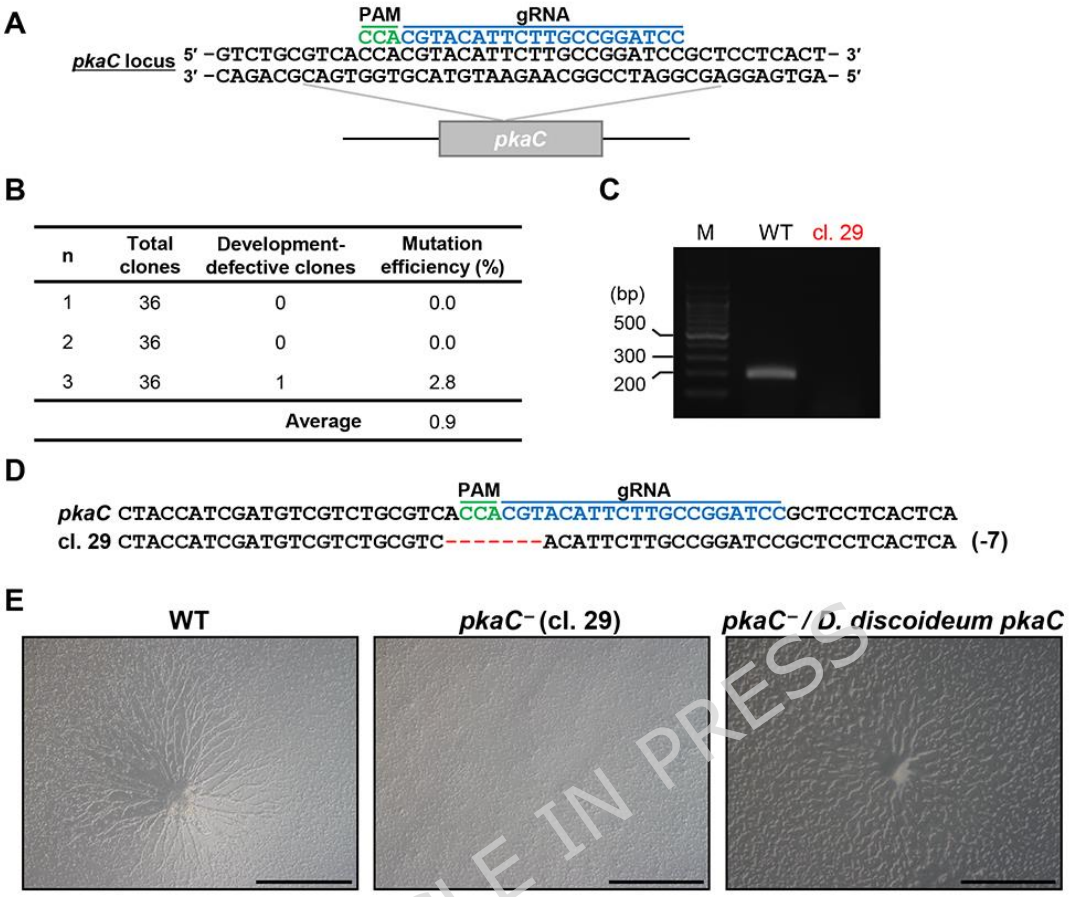

n	Total clones	Development-defective clones	Mutation efficiency (%)
1	36	0	0.0
2	36	0	0.0
3	36	1	2.8
		Average	0.9

Figure 2. Knockout of *pkaC* using an extrachromosomal CRISPR vector in *H. pallidum*.

(A) Schematic representation of the *pkaC* target region. (B) Proportion of clones exhibiting the development-defective phenotype. (C) Mutation detection PCR of the obtained clones. Clones highlighted in red represent PCR-positive candidates selected for sequencing. (D) Sequence analysis of the genomic region containing the target site. The target sequence is shown in blue, the PAM sequence in green, and mutations in red. Numbers in parentheses indicate the size of the mutation. (E) Developmental phenotypes of parental and mutant strains at 7 h after starvation. Scale bars: 0.5 mm.

ARTICLE IN PRESS

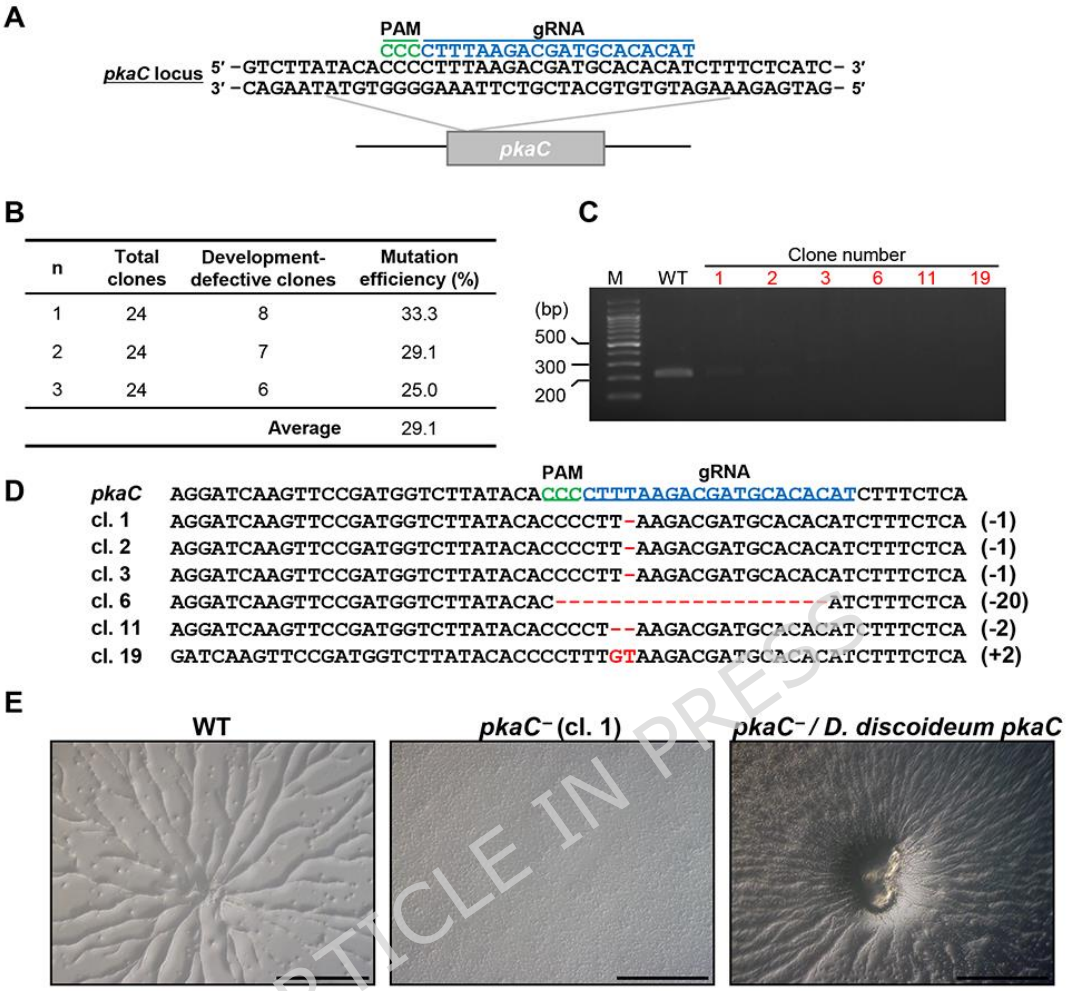

Figure 3. Knockout of *pka*C using an extrachromosomal CRISPR vector in *C. fasciculata*.

(A) Schematic representation of the *pkaC* target region. (B) Proportion of clones exhibiting the development-defective phenotype. In each of three independent experiments, 24 clones were examined for developmental phenotype. (C) Mutation detection PCR of a randomly selected subset of 6 development-defective clones. Clones highlighted in red represent PCR-positive candidates selected for sequencing. (D) Sequence analysis of the genomic region containing the target site. (E) Developmental phenotypes of parental and mutant strains at 7 h after starvation. Scale bars: 0.5 mm.

ARTICLE IN PRESS

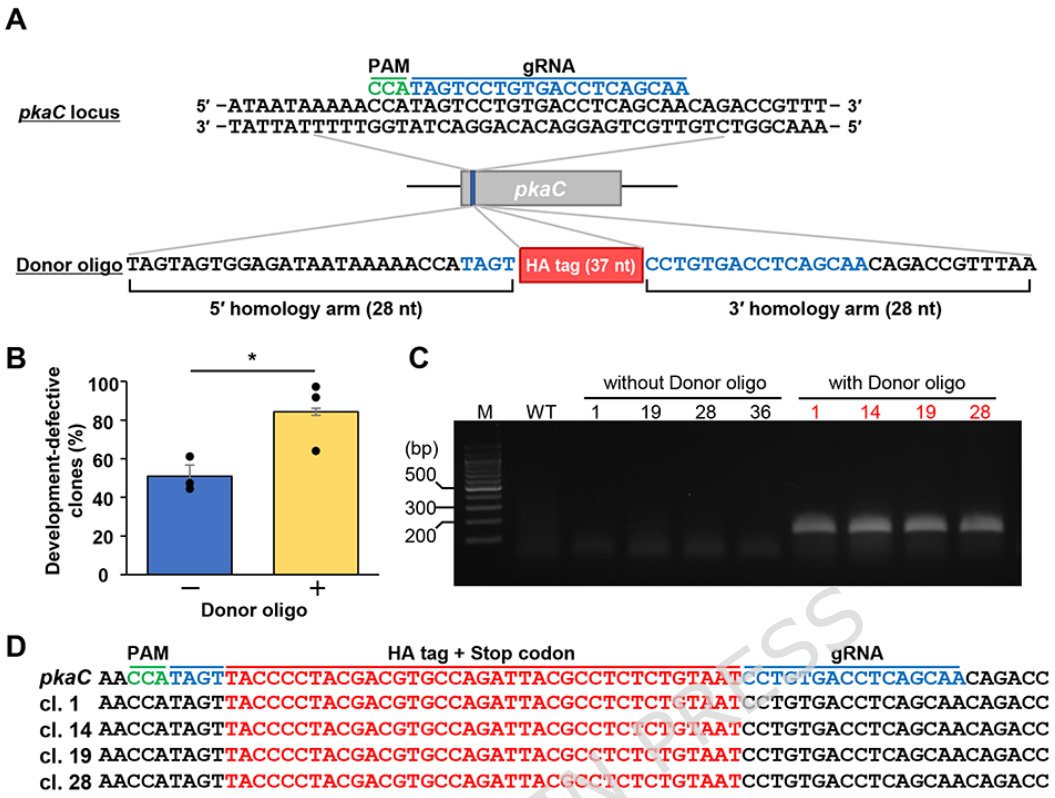

Figure 4. Knockout of *pkaC* using donor oligos in *D. discoideum*.

(A) Schematic diagram of the donor oligo design. The target sequence is shown in blue, the PAM sequence in green, and the 37 nt inserted sequences in red. Each side of the donor oligo was flanked by 28 nt sequences homologous to the *pkaC* locus. (B) Proportion of clones exhibiting developmental defects with or without donor oligos. In each of three independent experiments, 36 clones were examined, and the mean frequency ± standard deviation was calculated. Black dots represent individual replicates (n = 3). An asterisk indicates a statistically significant difference ($p < 0.05$, *t*-test). (C) Mutation detection PCR of the obtained clones. Primers were designed to amplify across the inserted sequence within the donor oligo and the downstream region of *pkaC*. Clones highlighted in red represent PCR-positive candidates selected for sequencing. (D) Sequence analysis of the genomic region containing the target site.

ARTICLE IN PRESS

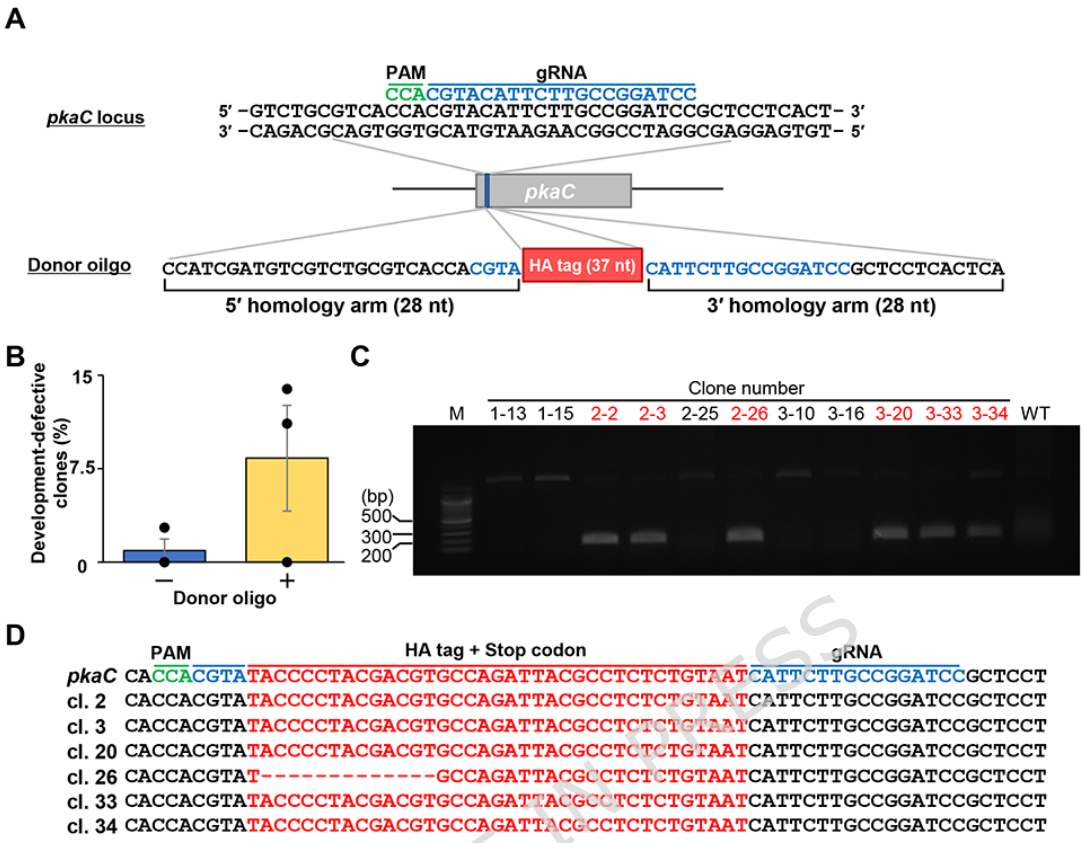

Figure 5. Donor oligo-mediated disruption of *pkaC* in *H. pallidum*.

(A) Schematic representation of the donor oligo. The target sequence is shown in blue, the PAM sequence in green, and the inserted tag (HA tag + stop codon). The 37-nt inserted tag was flanked on both sides by 28-nt sequences homologous to *pkaC*. (B) Disruption efficiency based on phenotypic analysis. Among 36 analyzed clones, those exhibiting developmental defects were counted, and the mean efficiency and standard deviation were calculated (n = 3). Black dots represent individual trials. A *t*-test revealed no statistically significant difference between the groups (p = 0.2195). (C) Mutation detection PCR. The target region was amplified using a primer complementary to the inserted tag together with a genomic primer. Successful insertion yielded a visible PCR band. Clones labeled in red were considered candidates and subjected to sequence analysis. (D) Sequence analysis of the target region.